APPLICATION OF NASTRAN TO LARGE SPACE STRUCTURES

T. Balderes, J. Zalesak, V. DyReyes
and E. Lee

Grumman Aerospace Corporation

SUMMARY

The application of NASTRAN to design studies of two very large-area lightweight structures is described. The first is the Satellite Solar Power Station, which would help meet the energy needs of the future, while the second is a deployable three hundred meter diameter antenna. A brief discussion of the operation of the SSPS is given, followed by a description of the structure. The use of the NASTRAN program for static, vibration and thermal analysis is illustrated and some results are given. Next, the deployable antenna is discussed and the use of NASTRAN for static analysis, buckling analysis and vibration analysis is detailed.

INTRODUCTION

The space programs of the future will involve the operation of very large structures in space. Current studies (References 1,2,4) are involved with various aspects of these projects, from assessing what type of space station would best serve as a prototype, to considerations of orbital construction techniques. A feature common to these investigations, is the large area structures involved. In fact a recent conference (Reference 3) sponsored by the Office of Aeronautics and Space Technology of NASA identified the principal driver in tomorrow's space technology as large area space structures. This paper describes the application of the NASTRAN program to this technology. The analysis of large space structures using the NASTRAN program is described. The first is the Satellite Solar Power Station which would help meet the energy needs of the future, and the second is a deployable 300 m (1,000 ft.) diameter antenna.

DISCUSSION

A. Solar Satellite Power Station

The Solar Satellite Power Station represents one of the energy sources of the future. Its feasibility, in terms of cost and needed technology, are being evaluated by Grumman in continuing studies that began five years ago. It has definite advantages over other alternatives such as ground based solar systems, nuclear fusion, and tapping the remaining coal deposits. Large energy storage systems are not required since operation is continuous, the necessary technology exists, and it represents an environmentally clean source. Moreover, initial economic studies indicate that power from an SSPS would be cost competitive with projected coal derived power.

The current SSPS design (Figure 1) consists of two large rectangular, solar panels, each measuring 6.5 km (4 miles) long by 4.7 km (2.9 miles) wide by 200 meters deep, interconnected by a single large mast. Solar reflectors consisting of lightweight plastic mirrors are arranged to concentrate solar energy onto the solar cells, effectively doubling the energy they receive (Figure 2). The electrical energy produced by the solar cells is transmitted in the form of d.c. power via a bus structure to the microwave antenna located between the two rectangular solar panels. The microwave antenna is .83 km (.52 miles) in diameter. The microwave beam is transmitted to earth where it is reconverted into electric power by an antenna-rectifier array and then fed into the power grid. The system under study would provide 5,000 megawatts of power at the receiving station, roughly enough to power a city the size of New York.

This entire concept requires the design of a large area lightweight structure that can not only support the solar cell blankets, concentrator mirrors, transmission bus system and antenna for the various loadings, but one that can be controlled in space.

A further constraint on the structure is that it be assembled or manufactured in space. This constraint becomes more obvious when the size and weight of the SSPS are considered. First, the structure is too large to be assembled in existing buildings (note that the vertical assembly building can be set between the truss structures that support the solar reflector panels). Second, handling on the ground would crush the lightweight structures. It has been determined that lifting a beam (made for a large space structure) longer than 18 m would exceed its allowable loading. Furthermore, estimates of the weight of the SSPS range as high as 18×10^6 Kg (40

million pounds). Noting that the Shuttle Orbiter's payload is 30. x 10^3 Kg (65,000 pounds), it becomes evident that a Heavy Lift Launch Vehicle that can carry 180. x 10^3 Kg (400,000 lbs.) will be needed. Moreover, to minimize the number of flights, manufacturing would be done in space, thus maximizing launch density. The concept of manufacturing in space has been under investigation and is being further studied under a current contract (Ref. 2). By using spools of material, structural elements would be made up with triangular cross-sections and then built up into complete beams, which would serve as truss members. The actual construction would be carried out using fabrication modules, as shown in Figures 3, 4 and 5. After the SSPS is completely assembled in low earth orbit, it would be transported to its final geosynchronous orbit with the use of a solar-electric propulsion system, as depicted in Figure 6.

The first operational SSPS could be built beginning in 1990 and would deliver power by the year 2000. Smaller systems (1 Mw) to demonstrate the concept and perform tests on the manufacturing techniques are being planned for the 1985-87 period.

The objective of this study was to perform structural and dynamic analyses of the SSPS structure for the purposes of:

- o providing elastic characteristics (natural frequencies, and mode shapes) of the structure for use in an analytical investigation of the elastic coupling between the SSPS attitude control system and the spacecraft's structural modes;

- o determining deflections and internal member loads for the various flight loading conditions in order to verify operational and structural integrity.

Figure 7 shows the general structural arrangement of the SSPS vehicle. The main structural framework for each of the two solar panels consists of a large diameter (80m) coaxial mast transmission bus, transverse power busses and nonconductive support structure. Shear loads are transmitted by prestressed tension-only wires. Structural continuity between the two solar arrays is supplied by the mast and dielectric structure running outboard of the antenna. The entire structure is aluminum alloy except for the carry-through structure surrounding the microwave antenna, which must have microwave transparency, and is glass/epoxy with quartz wire tension braces.

The structure of each solar array consists of 20 longitudinal (x-direction) truss girders inclined at 30 degrees from the x-z plane. Each truss girder consists of 20 meter deep members with shear stiffness provided by cross bracing cables. The mast is also considered part of the primary structure and is included in the analysis. The primary chordwise members are located at x = 630 m , x = 2109 m, x = 3588 m, x = 5607 m and x = 6546 m. These are made up of 20 m girders of various lengths. The lower members of the chordwise trusses are conductors that tie to the main bus and are considered to be structurally effective.

Each primary member (20m) consists of three 1-meter truss girder cap members held together by 1-meter truss girders spaced at 40m with cross bracing cables. The 1-meter truss girder is the basic structural member and is made up of three vee section caps braced every 3 meters. The mass breakdown for the SSPS is given in Table I.

The finite element model used in the NASTRAN analysis is shown in Figures 8, 9 and 10. An isometric view of the model is shown in Figure 8, while the top chord, bottom chord, concentrator wire bracing and the structure between top and bottom chords are shown in Figures 9 and 10. One half of the entire structure was modeled, with symmetric and antisymmetric boundary conditions applied. The symmetric model had 1,364 degrees of freedom and the antisymmetric had 1,342.

Using the above model, free vibration modes of the structure were obtained employing Rigid Format 3 and the Inverse power method. The two lowest symmetric and antisymmetric modes are shown in Figures 11 through 14.

The lowest mode is a symmetric bending mode with a frequency of 5.26 cycles/hour and would be excited by symmetric thruster forces such as those used in transport from low earth orbit to geosynchronous orbit. The second symmetric mode has a frequency of 14.14 cycles/hour and involves torsional motion. This is the lowest mode excited by the roll (rotation about x axis) control thrusters in their present configuration. The lowest antisymmetric mode involves torsional motion and has a frequency of 9.36 cycles/hour. The second antisymmetric mode is a bending mode (15.6 cycles/hour) which would be excited by the pitch (rotation about y axis) control thrusters.

In order to perform the transient response analysis, the number of degrees of freedom was reduced by employing the Guyan reduction technique. The symmetric model was reduced to 174 degrees of freedom and the antisymmetric to 162. A comparison of the model data revealed that the first 15 frequencies agreed to within 10% and the lowest 4 frequencies to within 3%. The NASTRAN

program, however, was not used for the frequency and transient response because of problems with Rigid Format 11 in level 15.5. The FRRD module would not execute, and it was found that for problems using multipoint constraints an overlay problem existed. Although the problem was eventually corrected, the project schedule did not allow the use of NASTRAN. Alternate in-house programs were used.

Transient response analyses were carried out for control forces and transport forces (transport from LEO to geosynchronous orbit). The response analysis due to attitude control and station keeping yielded deflections and maximum member loads that are well within the allowables. Thrust forces related to 90, 150 and 365 day transit from LEO to gyosynchronous orbit indicated that the bending moments were within the allowables for the 365 day trip.

The SSPS is exposed simultaneously to solar heating and to electrical heating in the electrical transmission buses which are structural members. A thermal stress analysis was performed to determine if the distortions are severe enough to degrade the efficiency and to determine the thermal stresses in the structure. Two thermal conditions were considered. Electrical heating in the mast (resulting in a 150°C rise in temperature) while the SSPS is in the earth's shadow; electrical heating in the mast when the SSPS is exposed to the sun. Deflections due to these two thermal conditions are shown in Figure 15. The maximum deflection for both cases occurs at the tip of the mast and is 50m for the first case and 21m for the second. Both of these represent less than 1° slopes which is the limit specified on distorations to assure sufficient sunlight impinging on the solar cells so that cell efficiency is not degraded. Maximum loads in the structure for these two conditions were within allowables, except for some cable loads (providing shear ties in trusses) which had high compressive loads. Providing alternate load paths or sufficient preloading of the cables must be considered.

B. 300 Meter (1,000 ft.) Diameter Deployable Antenna

The second large structure, designed to operate in space, where NASTRAN was the analytical tool applied is the 300m diameter deployable antenna. The antenna would operate in an earth orbit and would be subjected to gravity gradient, solar pressure, control loads and temperature distributions. The configuration of the structure is shown in Figure 16. The structure consists of 72 rim members (each 13m (43') long) connected end to end to form the 300 meter diameter rim. The rim is supported by two sets of 36 cables (under tension) the forestays and backstays, connecting to alternate points on the rim. A gore structure, supporting antenna elements, is positioned in the plane of the rim and is also under tension. The upper systems module is

placed at the end of the mast which is 750 meters (2,500 ft.) from the plane of the rim. The rim elements consist of 13.3 cm ($5\frac{1}{4}$ in.) diameter tubes of graphite epoxy with a thickness of .038 cm (.015 in.). The forestays and backstays are unidirectional graphite epoxy tapes, the former being 2.54 cm (1.0 in.) wide and .03 cm (.012 in.) thick and the latter 1.9 cm (.75 in.) wide and .005 cm (.002 in.) thick. The mast structure, shown in Figure 17a is a graphite epoxy truss structure using three cap members, transverse support members and diagonal ties. The gore is made up of 72 triangular sectors, two of which are shown in Figure 17b, constructed of perforated aluminum sheet.

The entire structure is designed so that it can be packaged in the Space Shuttle Orbiter for transport to low earth orbit. There it would be deployed and transported to a geostationary orbit. The deployment procedure for a similar antenna is depicted in Figure 18. In the packaged configuration, the mast is collapsed, and the rim members are lined up axially one next to the other around the canister containing the mast. The rim elements are hinged, the top to the rim member to the left and the bottom to the rim member on the right. After the mast has extended, the rim members begin to deploy, moving outward radially from the mast and rotating about the center of their lengths. In the process the circle formed around the mast by the inclined rim members gets larger. In the deployed position each rim member is horizontal and has rotated 90° about a radial line outward from the mast. The NASTRAN analysis helped to establish guidelines for the design of the structure, which was required to hold stringent dimensional tolerances. The following analyses were performed using NASTRAN: static analysis with pretension loads; buckling analysis and vibration analysis.

The finite element model is shown in Figures 19 and 20. The rim and mast were modeled with bar elements, the forestays and backstays with rod elements and the gore sectors with membrane triangles.

The static analysis involved determining the deflections and member loads of the structure due to the operational pretension loads in the stays and gore. For all the static analysis, the structure was supported in a statically determinate fashion and Rigid Format 1 was used. The stays were pretensioned by applying a load of 89.09 N (20.0316) in the z direction at node 146 (see Figure 19), while the gore was pretensioned by applying inward radial loads of 23.6 N (5.32 lb.) at the apex of each triangular sector. The resulting member loads and deflections are given in Table II. Note that points on the rim to which forestays are attached have different deflections from points to which backstays are attached due to the different loads in the forestays and backstays. Deflections and members loads in the prestressed structure due to, in one case a broken forestay, and in the second case a broken

backstay were also obtained. Since the structure is not symmetric about the gore plane, a broken frontstay and a broken backstay will have different effects. Member loads for both cases did not change appreciably from their values under nominal prestress conditions. The resulting deflections of points on the rim in the radial and axial directions, are shown in Figures 21 and 22. Note that the distortions are very local being confined to a maximum of eight neighboring node points on the rim.

Under the action of the pretension loads, the rim experiences a compressive load of 413.7 N (93 lbs.), and hence may be subject to an instability condition. This was investigated by employing Rigid Format 5 to obtain the buckling loads of the structure. The mode shape corresponding to the lowest buckling load (1089.8 N (245 lbs.) compression in the rim) is shown in Figure 23. For this mode the structure behaves as a series of beams with length equal to twice the length of a single rim member supported at the center by a spring (and nct as a ring on a continuous elastic foundation).

The vibration analysis of the antenna was carried out to obtain the free-free modes which would then be used in a subsequent analysis to determine the structural response due to control forces. The finite element model was the same as that used for the static analysis. The mass of the structure was lumped at the nodes. The mass of the gore material in the plane of the rim (thin disk) was distributed by lumping 50% of its mass at the nodes of the rim, and the remaining 50% on the mast node (thus preserving the mass moments of inertia). Some of the lower modes are shown in Figures 24 and 25. Note that the lowest modes involve bending of the mast, while higher modes involve bending of the rim.

CONCLUSIONS

The application of NASTRAN to the analysis of two very large-area lightweight space structures has been described. The broad capability and large capacity of the NASTRAN program make it well suited for the analysis tasks required in the design studies. Static, buckling and free vibration analyses were carried out without any problems. Difficulties were, however, encountered in running Rigid Format 11 (Frequency response analysis) and an alternate program was used. The results of the analysis indicated the feasibility of the designs and helped pinpoint problem areas requiring design modifications.

From an overall viewpoint, the NASTRAN program is one of the major structural analysis tools at Grumman and is used on many other projects. On the average, it represents 30% of computer time used for structural analysis with additional usage (approximately 1/3 to 1/2 of the above computer time) attributed to dynamic analysis. Its broad applicability will insure its use on future work, it must however be maintained and updated on a continuing basis.

REFERENCES

1. Space Station Systems Analysis Study; Grumman Contract No. NAS-8-31993.

2. Orbital Construction Demonstration Study; Grumman Contract No. NAS-9-14916

3. OAST Summer Workshop Proceedings; Structures and Dynamics Panel; Aug. 3-16, 1975, Conducted at Madison College, Harrisonburg, Va.

4. Second interim report, space-based solar power conversion delivery systems study; vol 2 Engr Analysis of Orbital Systems; in support of contract No. NAS 8-31308 to NASA/MSFC.

TABLE I

SSPS MASS DISTRIBUTION

ITEM	MASS	
	Kg x 10^6	lb. x 10^6
SOLAR CELL BLANKETS	7.82	17.25
SOLAR CONCENTRATORS	1.23	2.71
NONCONDUCTING STRUCTURE	2.33	5.14
CONDUCTING BUSSES	.27	.59
MAST	.62	1.37
MICROWAVE ANTENNA	5.55	12.23
ROTARY JOINT	.17	.37
CONTROL SYSTEM	.036	.08
TOTAL	18.02	39.74

TABLE II

MEMBER LOADS & DEFLECTIONS DUE TO

PRETENSION LOADS IN DEPLOYABLE ANTENNA

LOADS IN MEMBERS		
Rim - axial compression -	416.8 N	(93.7 lbs.)
Forestays - axial tension -	22.24 N	(5.0 lbs.)
Backstays - axial tension -	4.804 N	(1.08 lbs.)
Gore - average σ_{rr} -	620 kPa	(90 psi)

DEFLECTIONS	Δr		Δz	
Points on Rim to which forestays are attached	-.386 cm	-.152 in.	-6.63 cm	-2.61 in.
Points on Rim to which backstays are attached	-.335 cm	-.132 in.	-7.08 cm	-2.79 in.

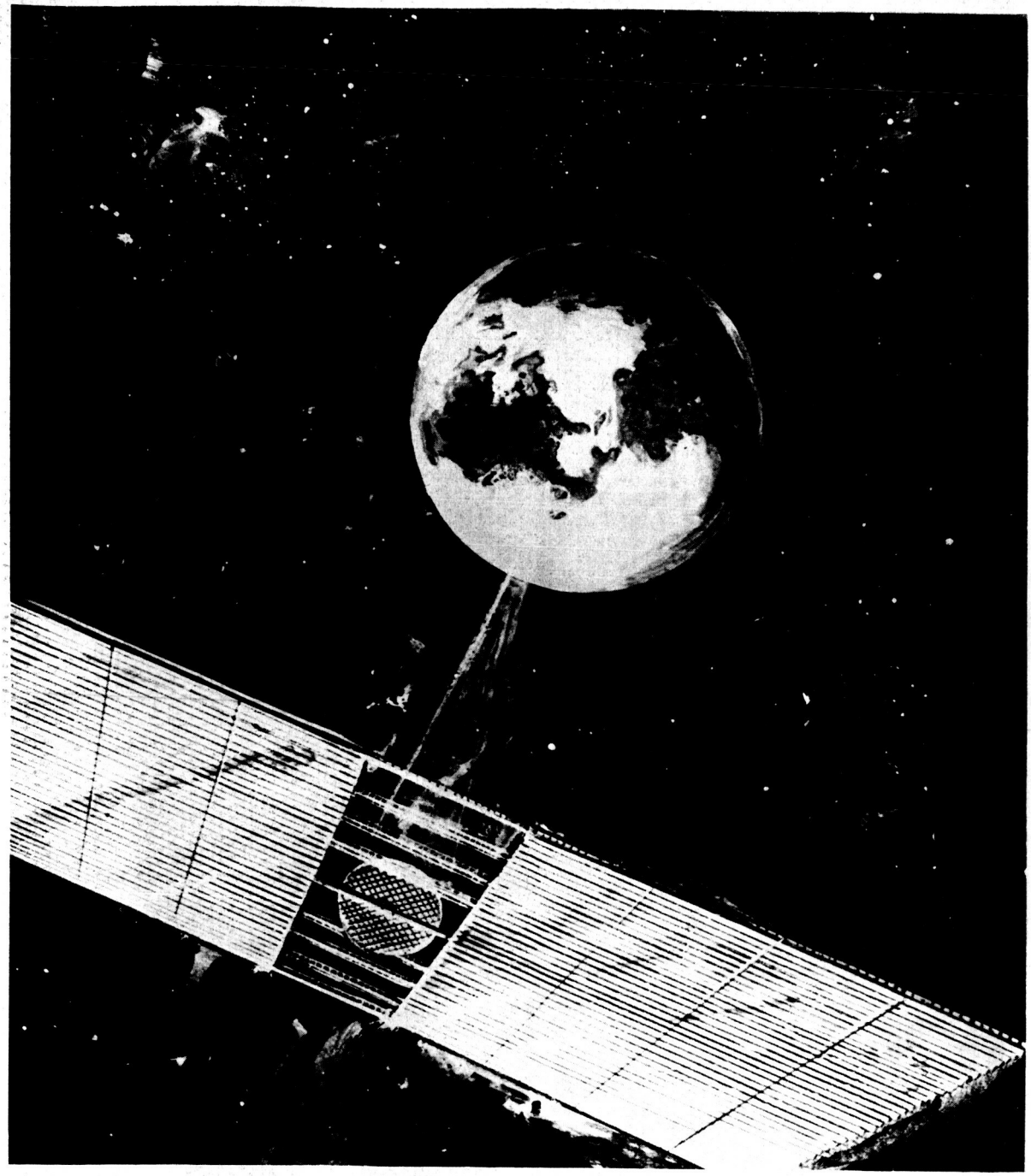

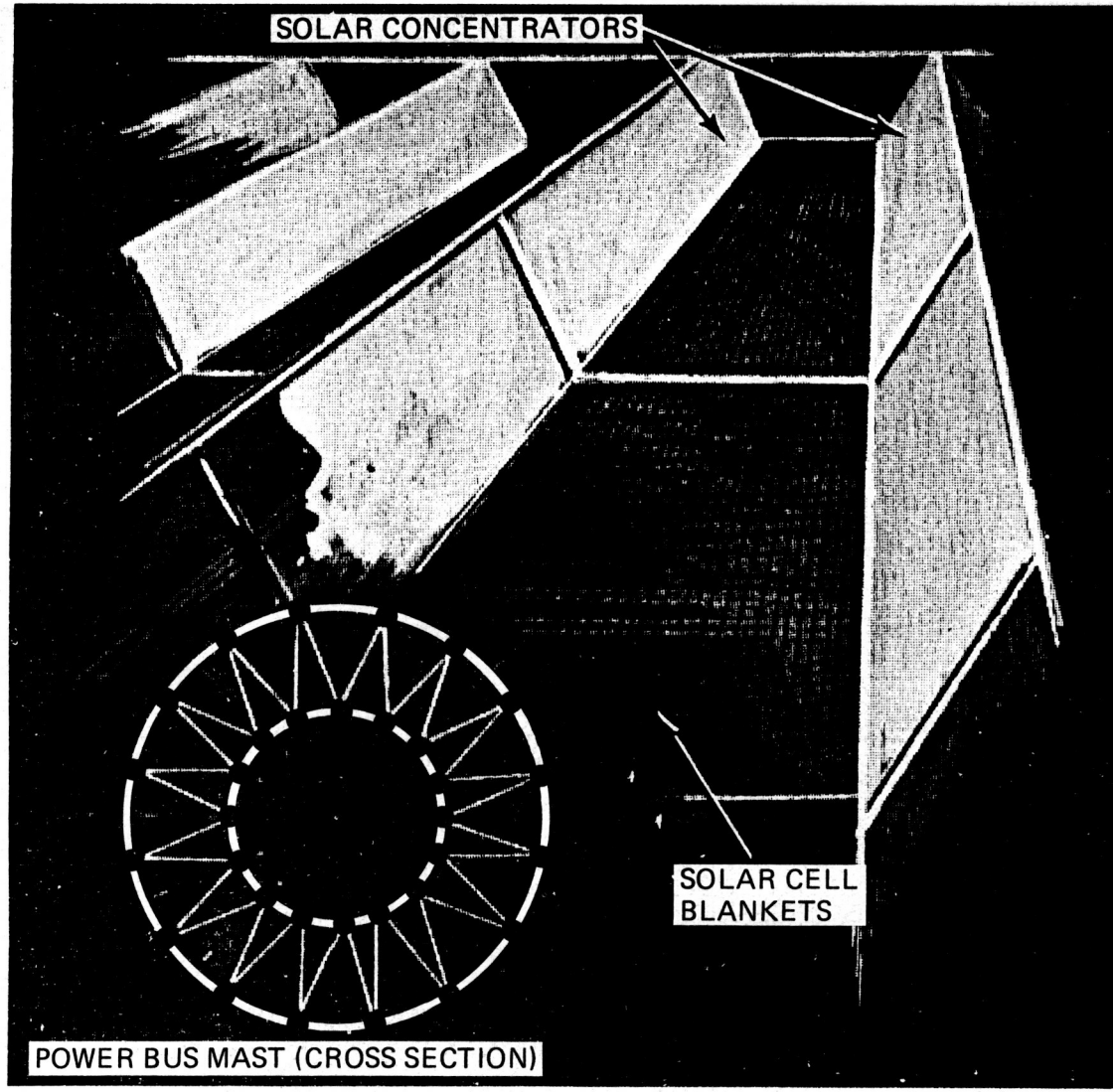

Fig. 2 Solar Panel Detail

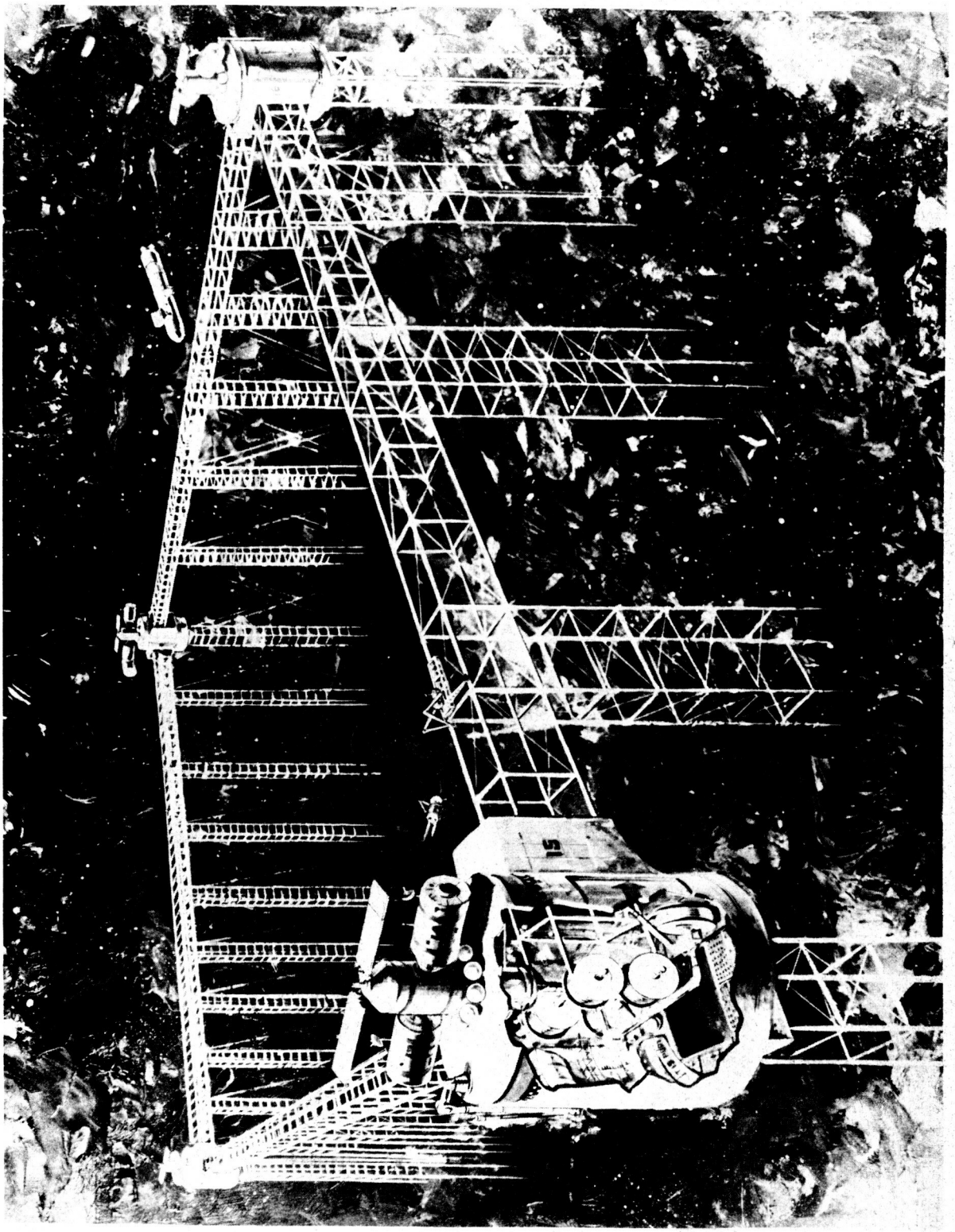

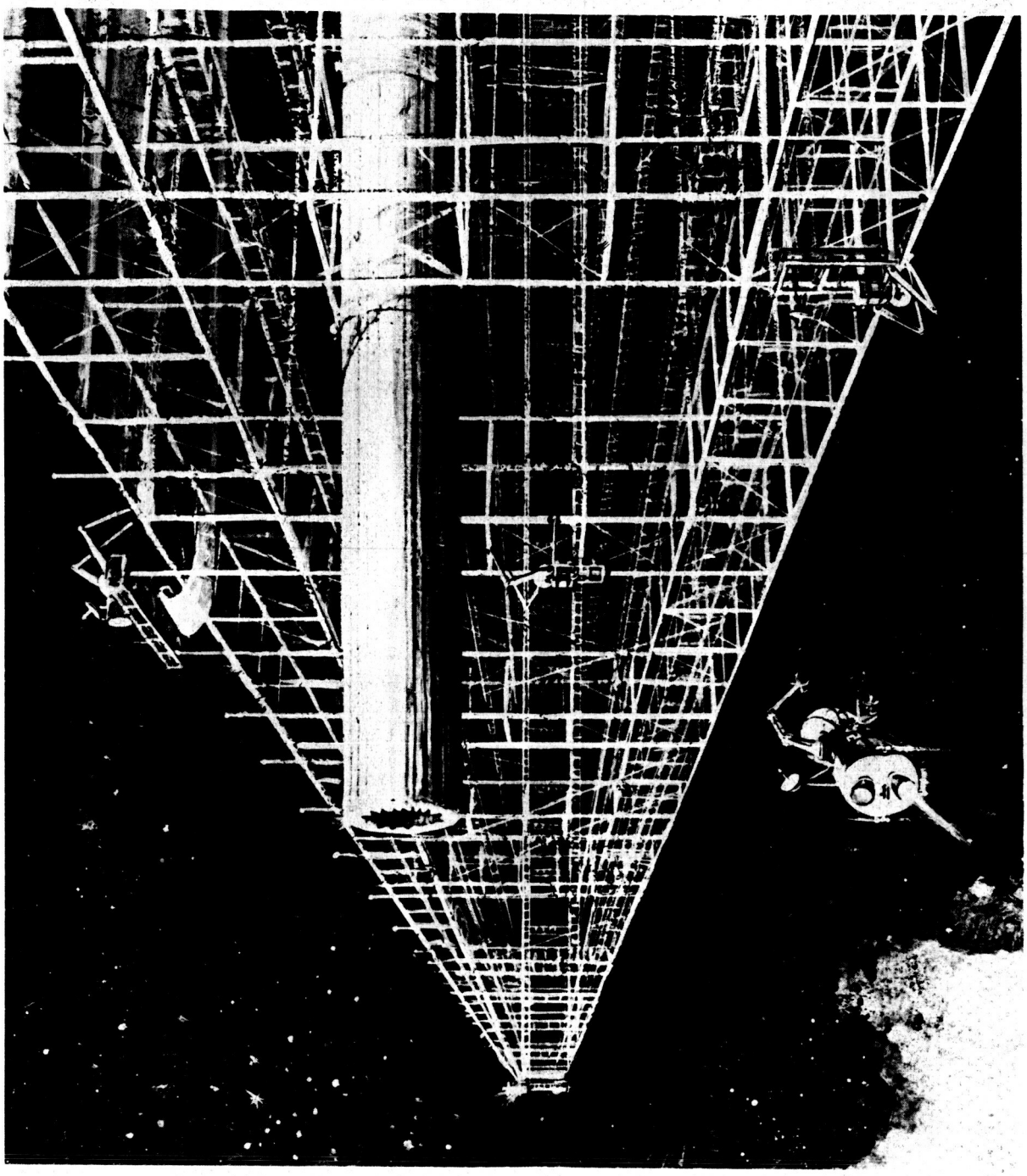

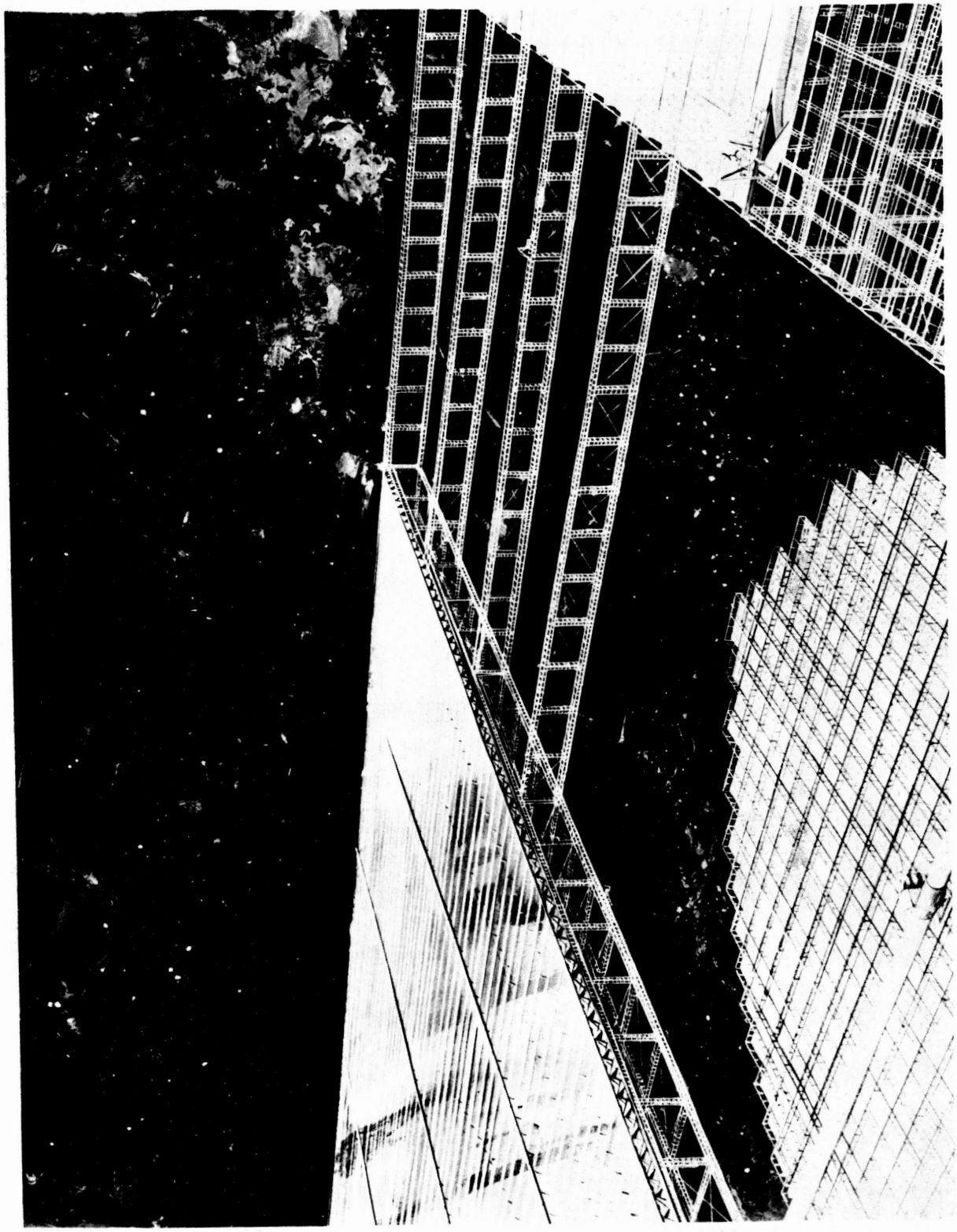

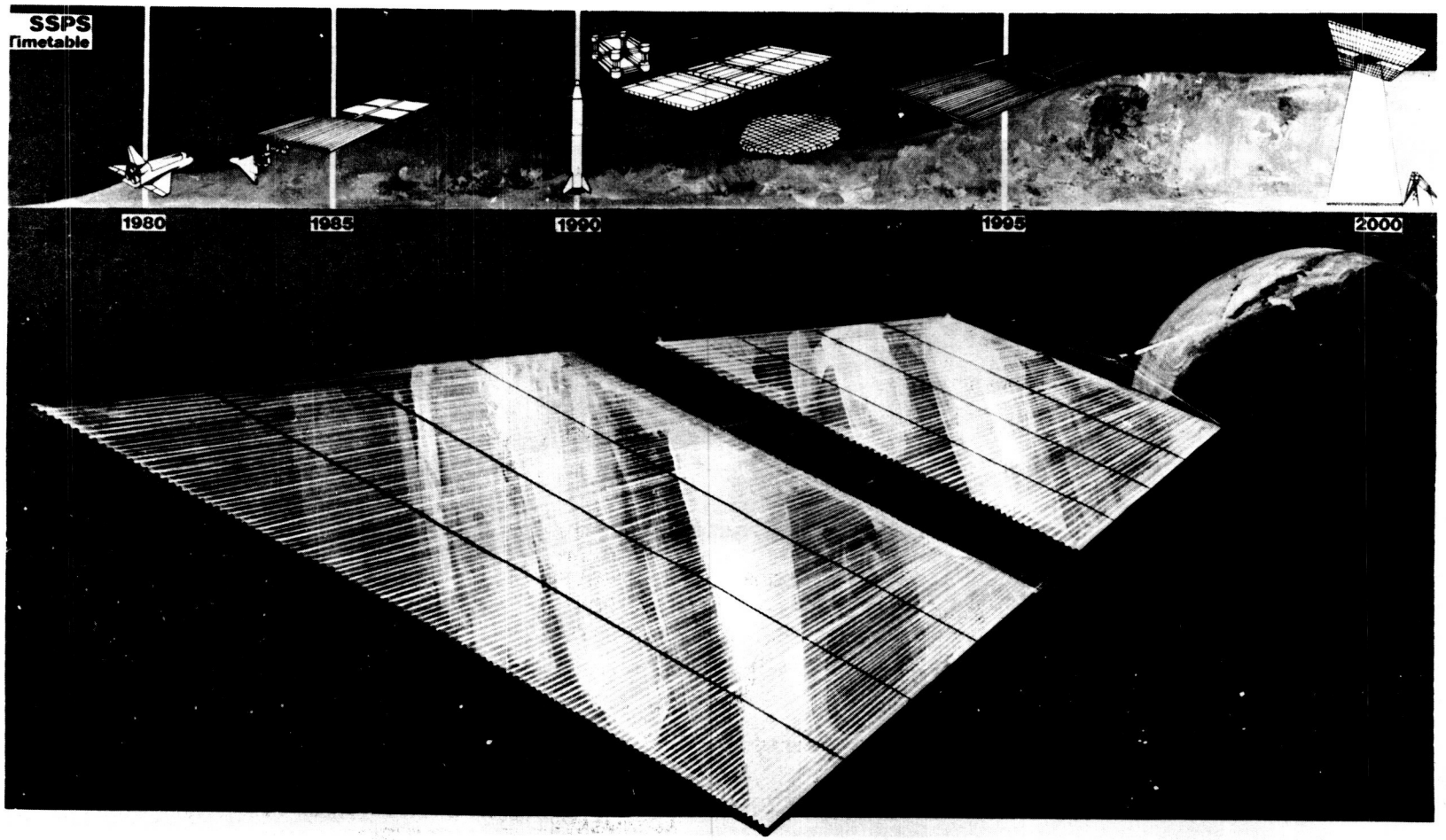

Fig. 6 Transport of SSPS From LEO to Geosynchronous Orbit

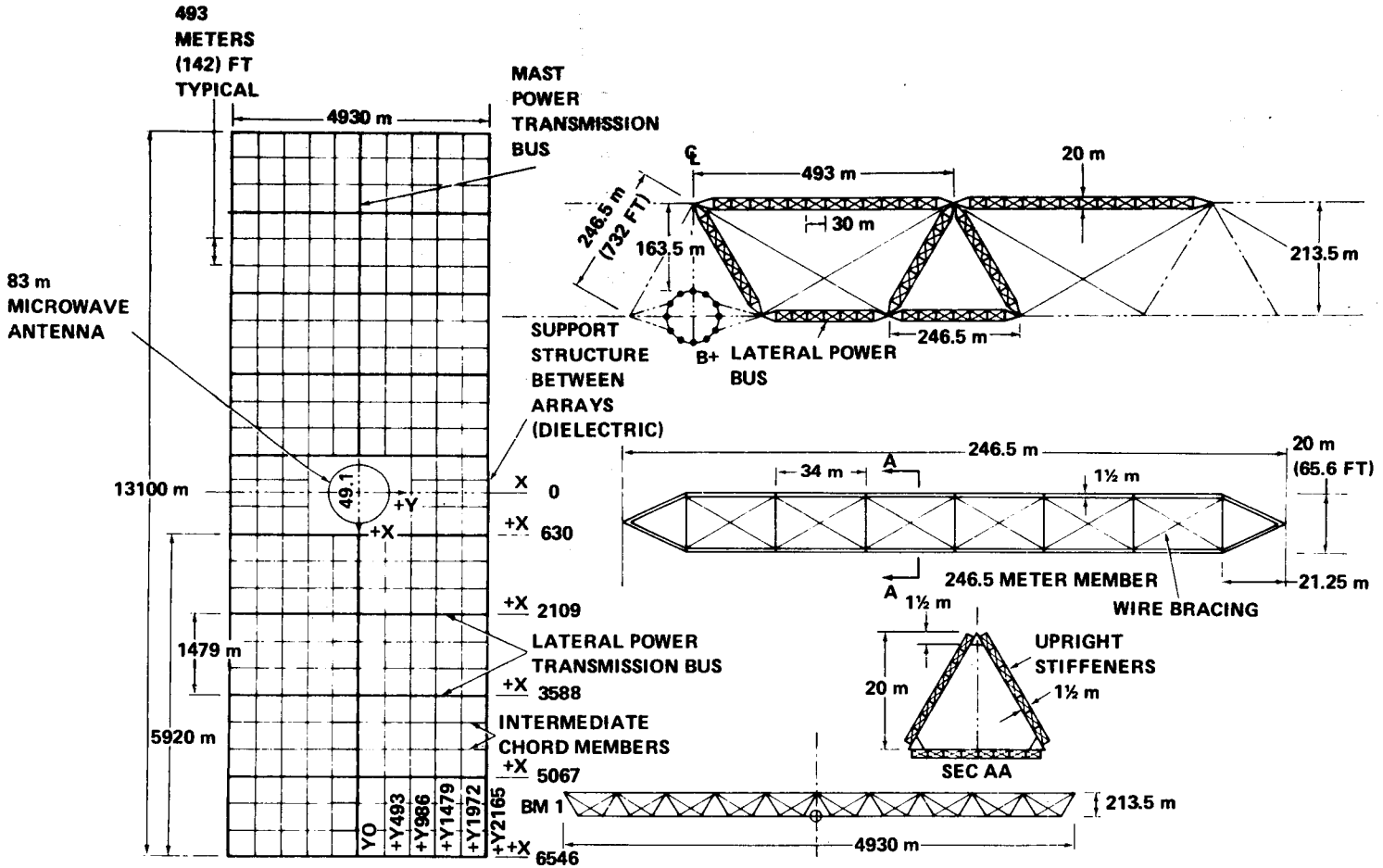

Fig. 7 SSPS Structural Arrangement

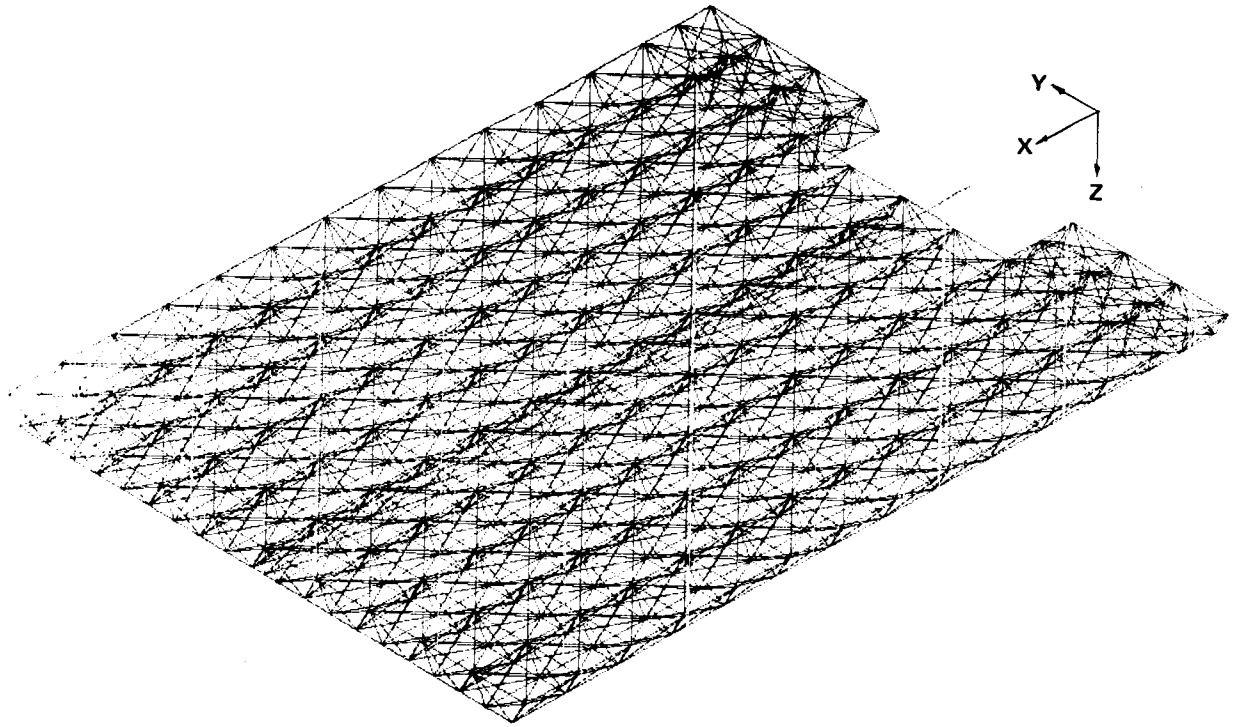

- HALF STRUCTURE CONSISTS OF 1127 MEMBERS AND 462 NODES
- SATELLITE WEIGHT DISTRIBUTED AS LUMPED MASSES AT NODE POINTS
- TENSION-ONLY WIRES REPLACED BY TENSION/COMPRESSION STRUTS
- PROPRETIES

WT = 18.02×10^6 KG (39.74×10^6 LB)

$X_{CG} = 0$

$Y_{CG} = 0$

Z_{CG} = 261.6M (858.3 FT)

$I_X = 2.445 \times 10^{13}$ KG-M^2 (1.803×10^{13} SLUG-FT^2)

$I_Y = 1.883 \times 10^{14}$ KG-M^2 (1.389×10^{14} SLUG-FT^2)

$I_Z = 2.118 \times 10^{13}$ KG-M^2 (1.5652×10^{14} SLUG-FT^2)

Fig. 8 Finite Element Model

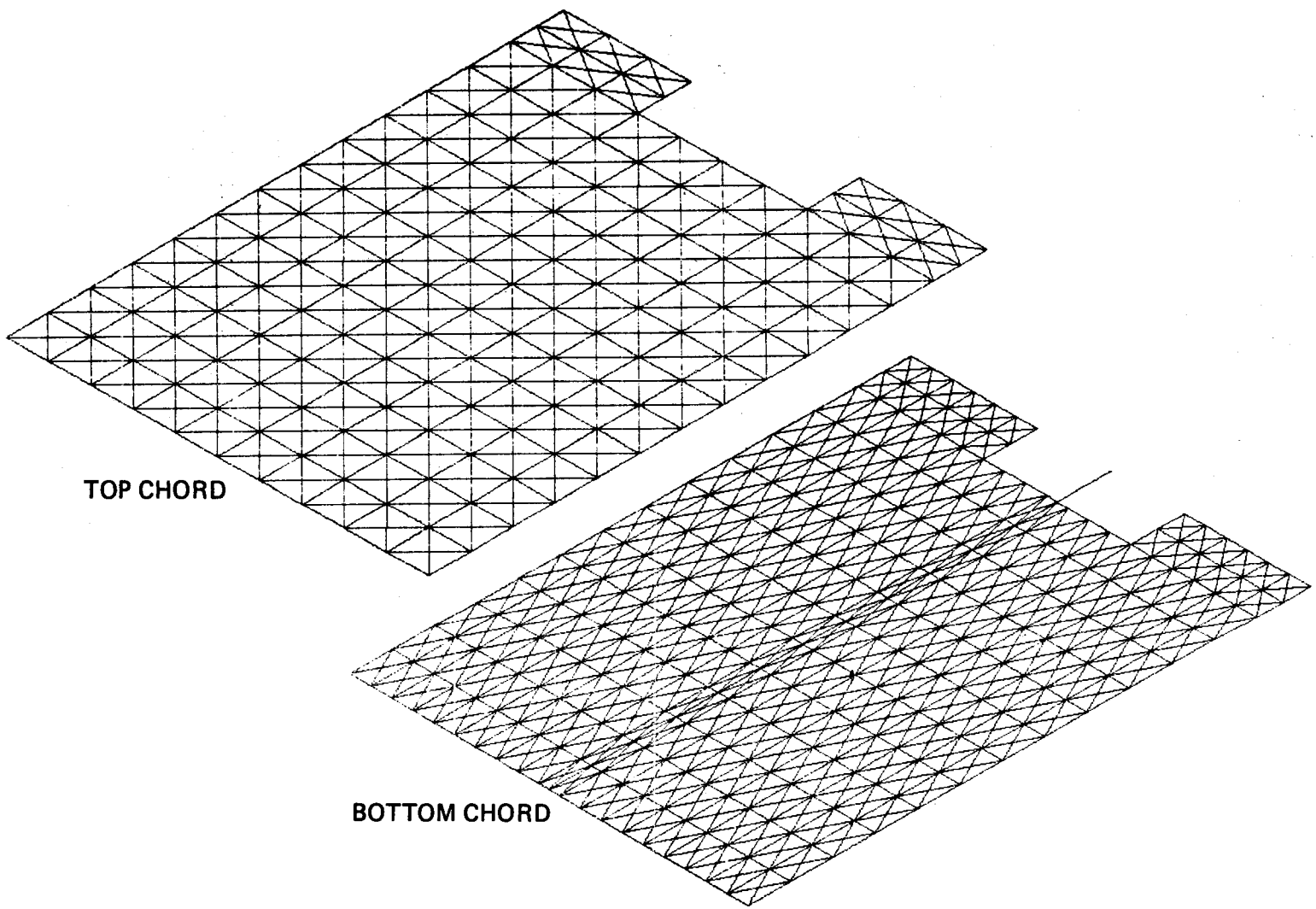

Fig. 9 Finite Element Model

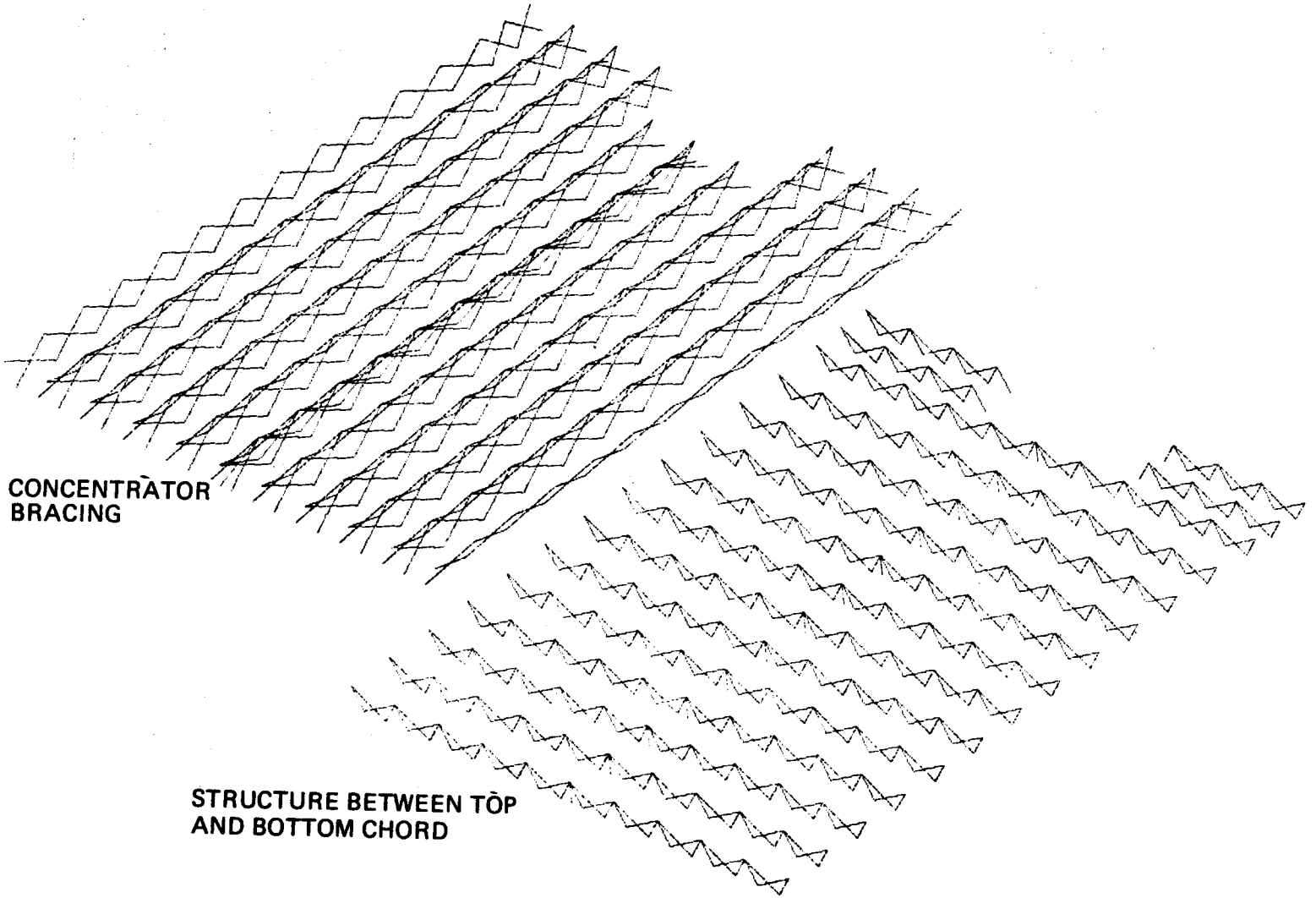

Fig. 10 Finite Element Model

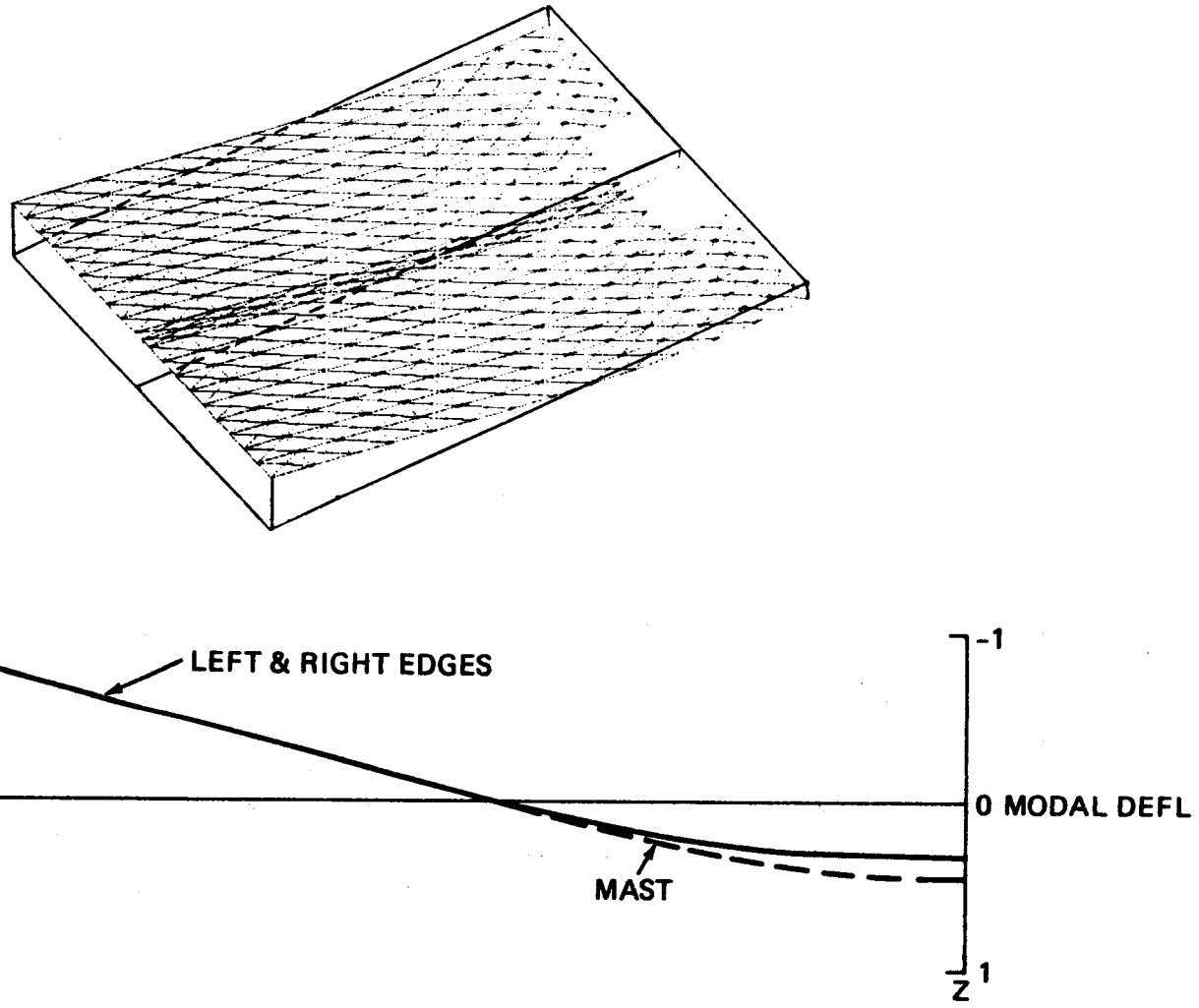

Fig. 11 SSPS Symmetric Mode - First Bending, Frequency = 5.26 C/Hr

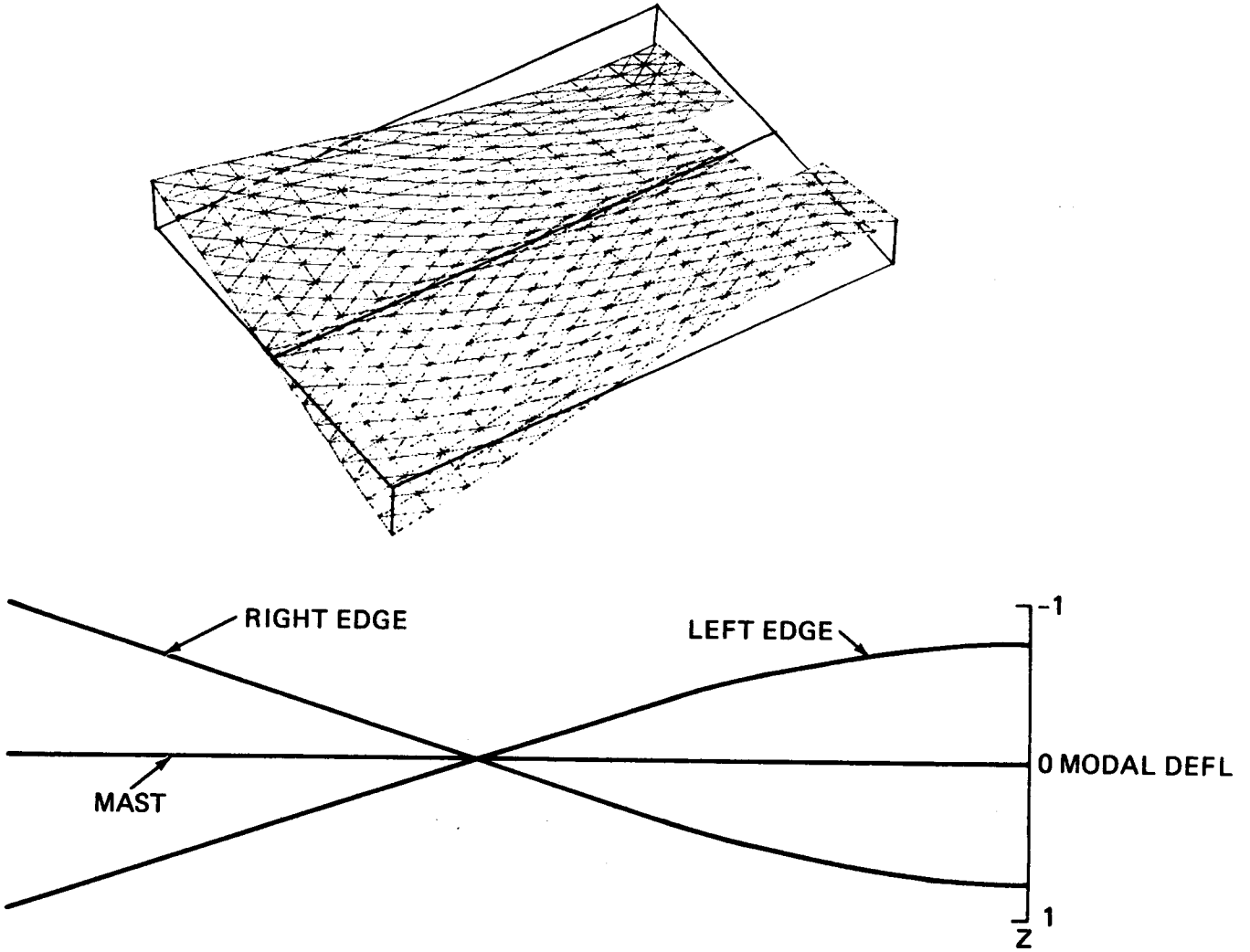

Fig. 12 SSPS Symmetric Mode - First Torsion, Frequency = 14.14 C/Hr

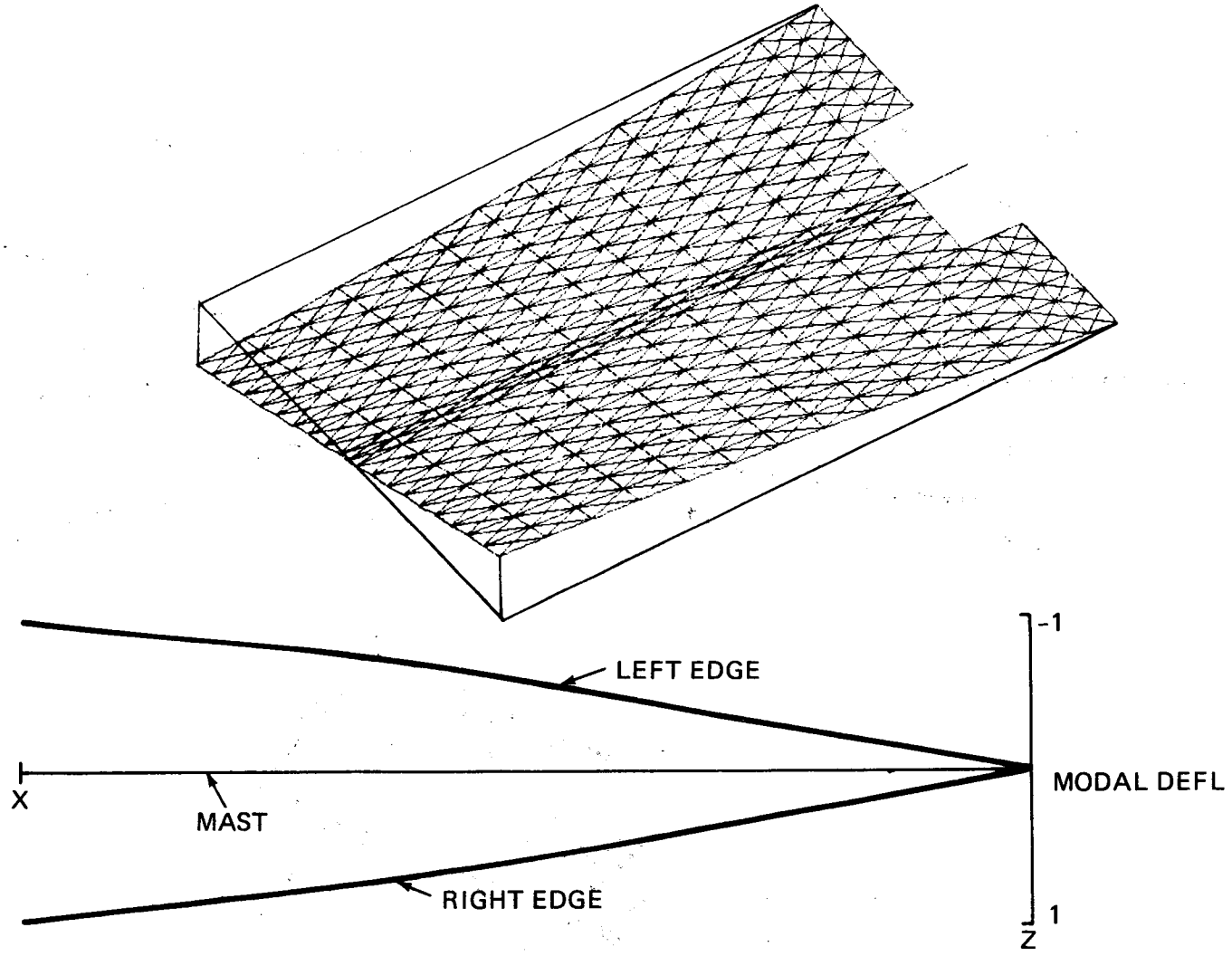

Fig. 13 SSPS Antisymmetric Mode - First Torsion, Frequency = 9.36 C/Hr

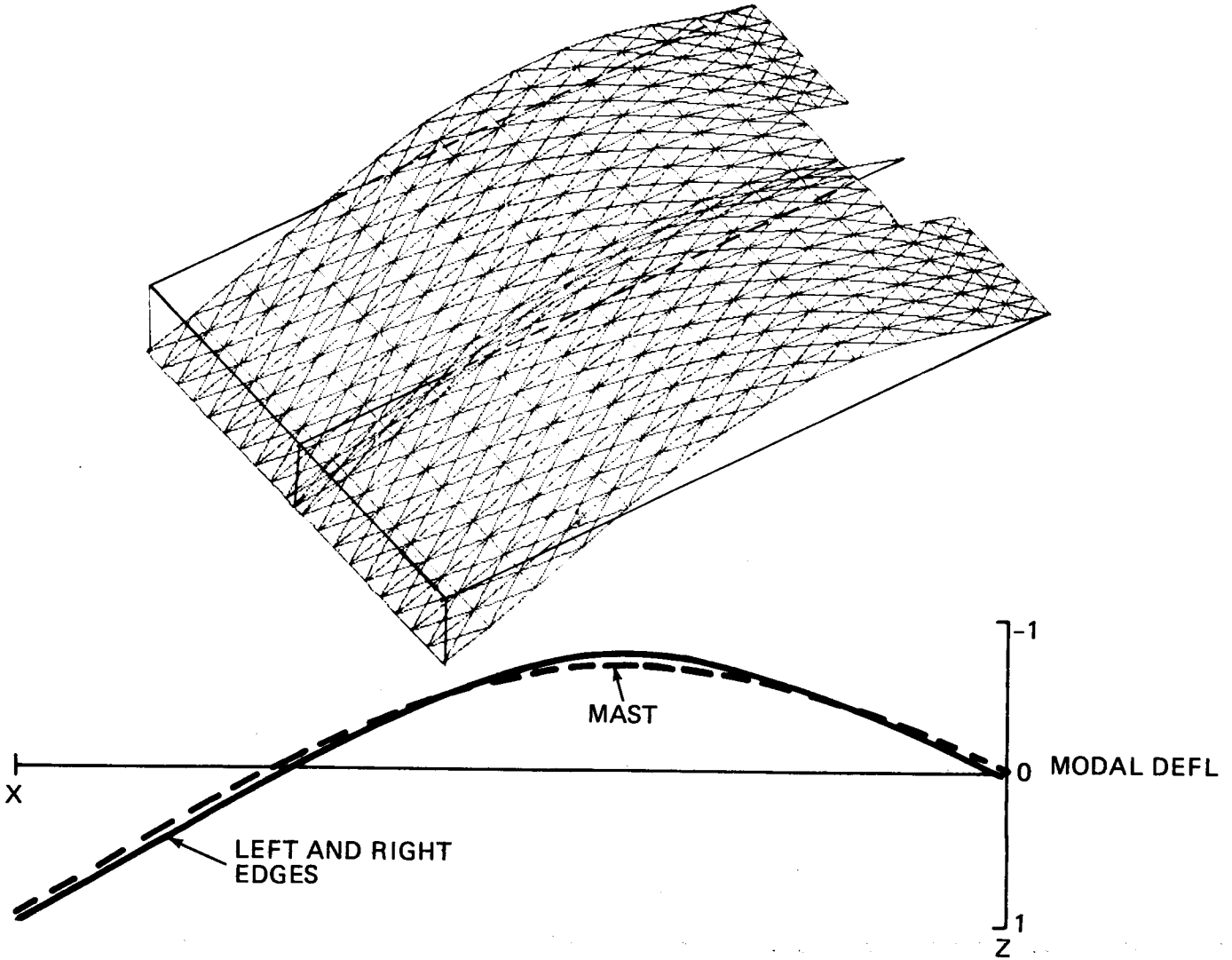

Fig. 14 SSPS Antisymmetric Mode - First Bending, Frequency = 15.65 C/Hr

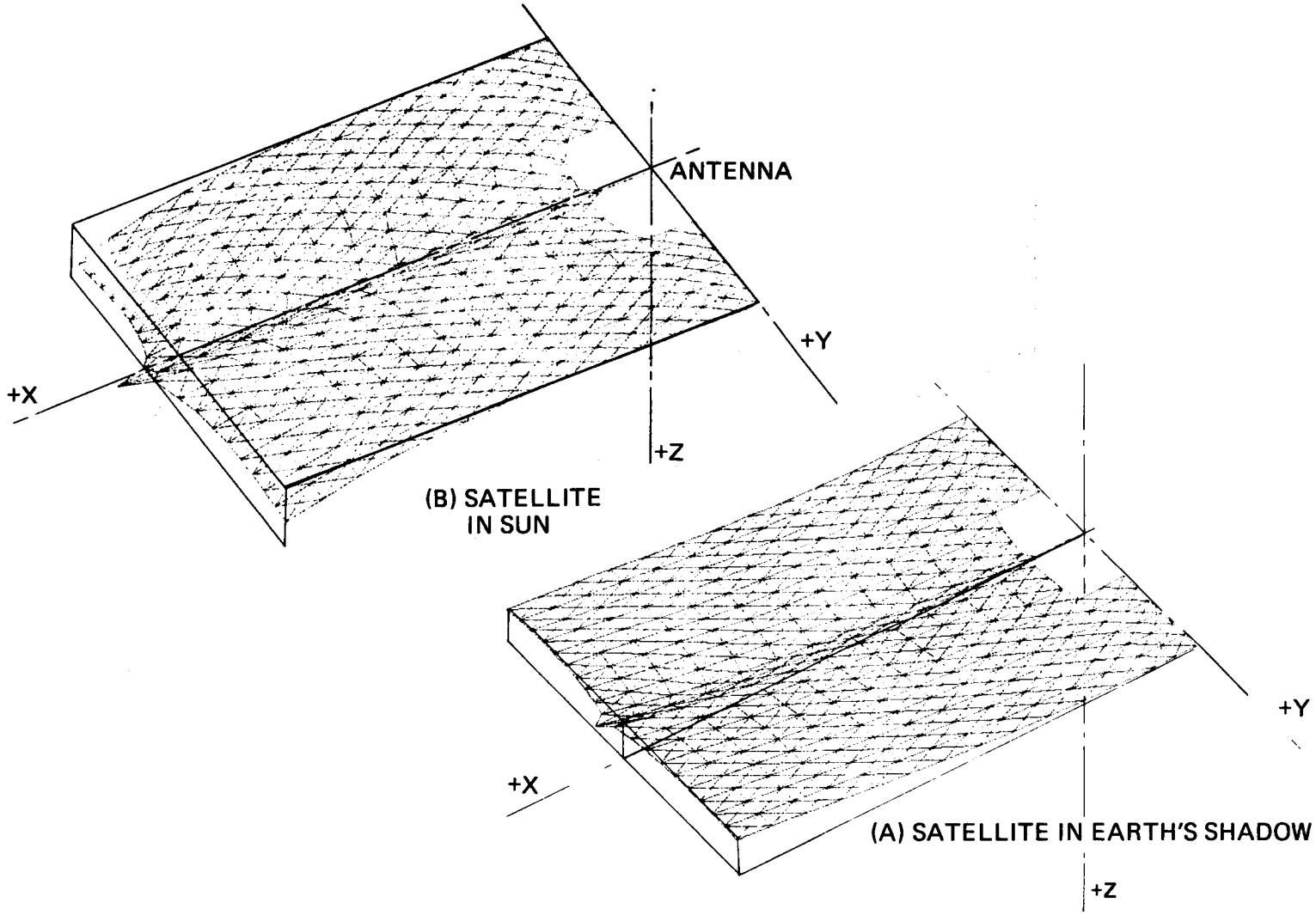

Fig. 15 Deflections Due to Thermal Conditions

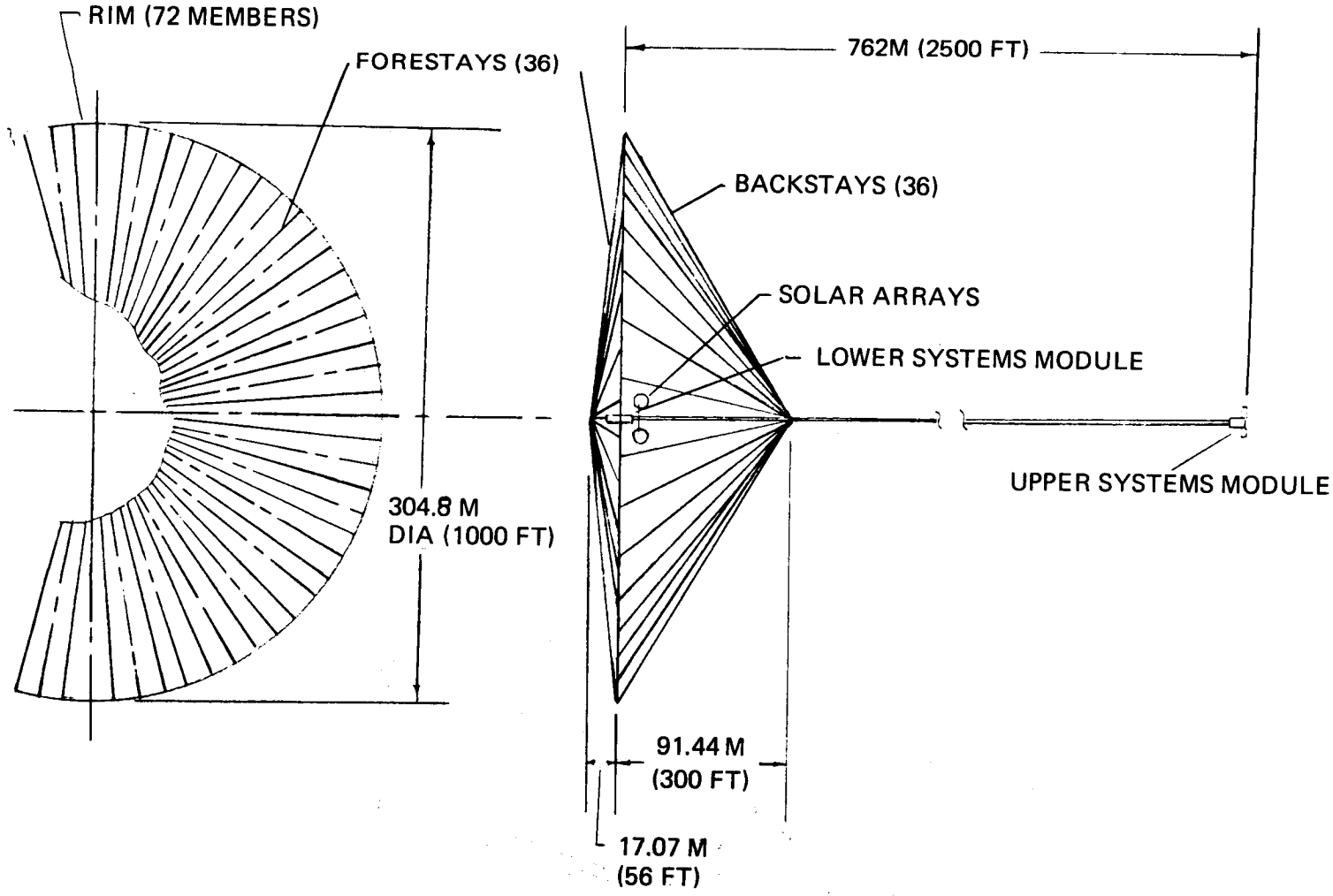

Fig. 16 Configuration of 300M (1000 FT.) Diameter Deployable Antenna

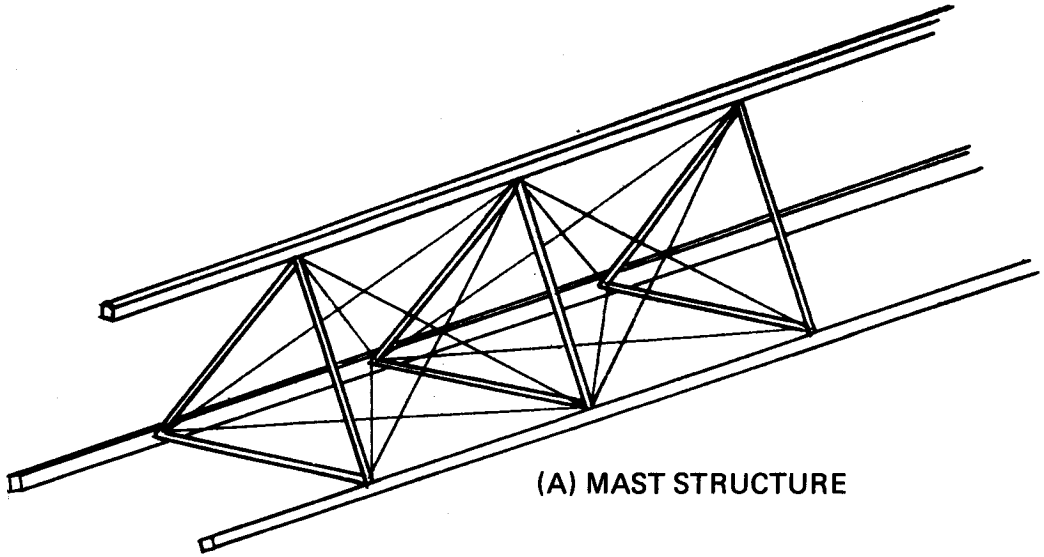

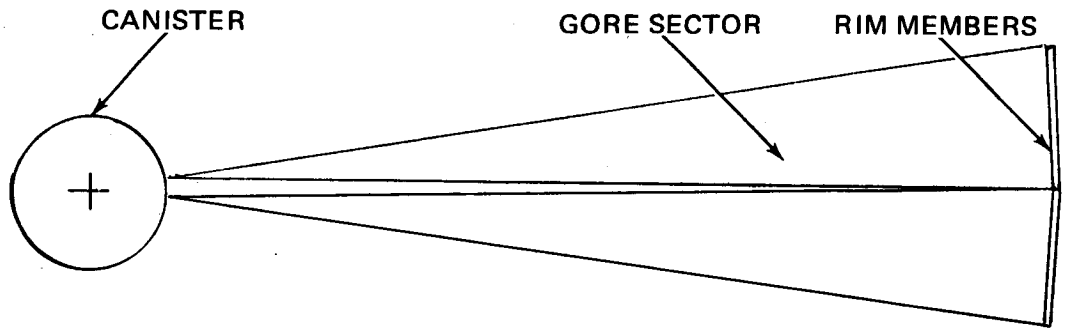

(B) GORE SECTORS

Fig. 17 Structural Components of Antenna

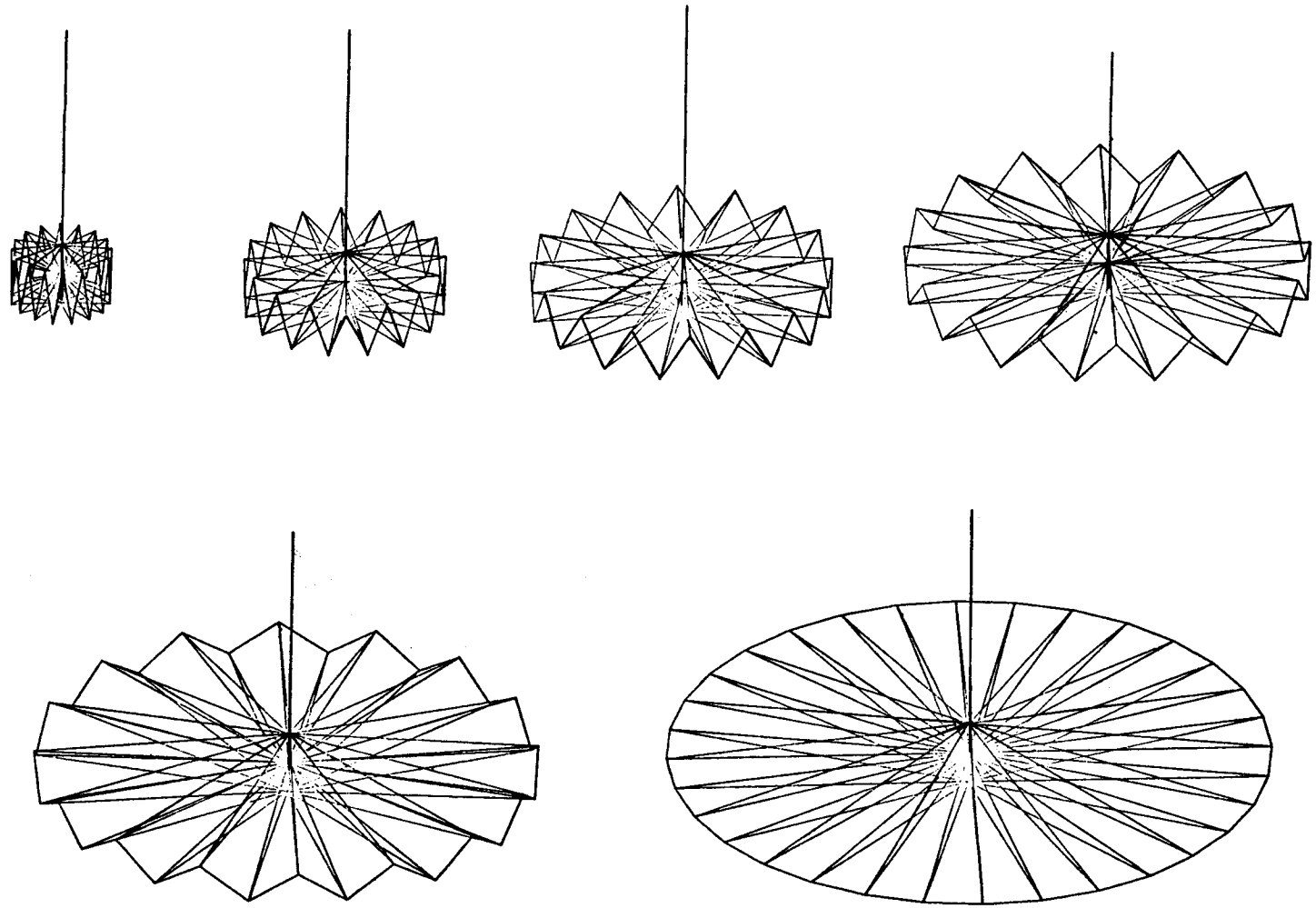

Fig. 18 Antenna Deployment Procedure

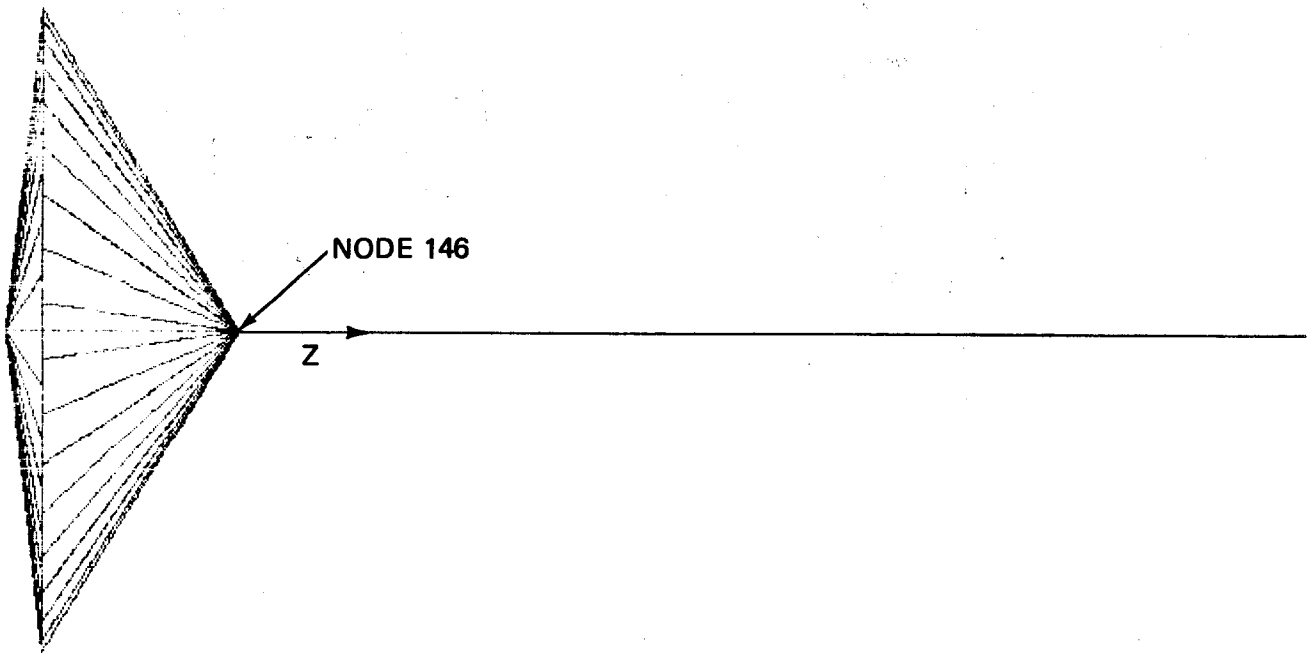

Fig. 19 Finite Element Model

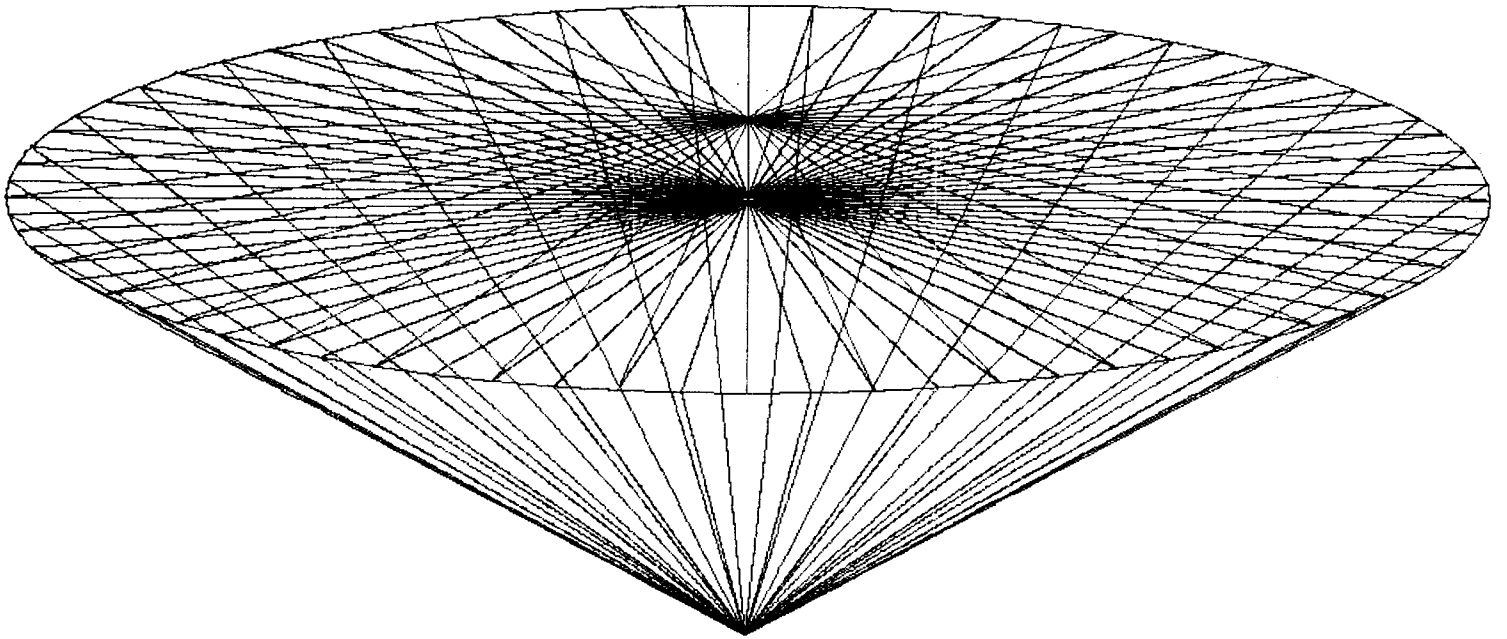

Fig. 20 Finite Element Model

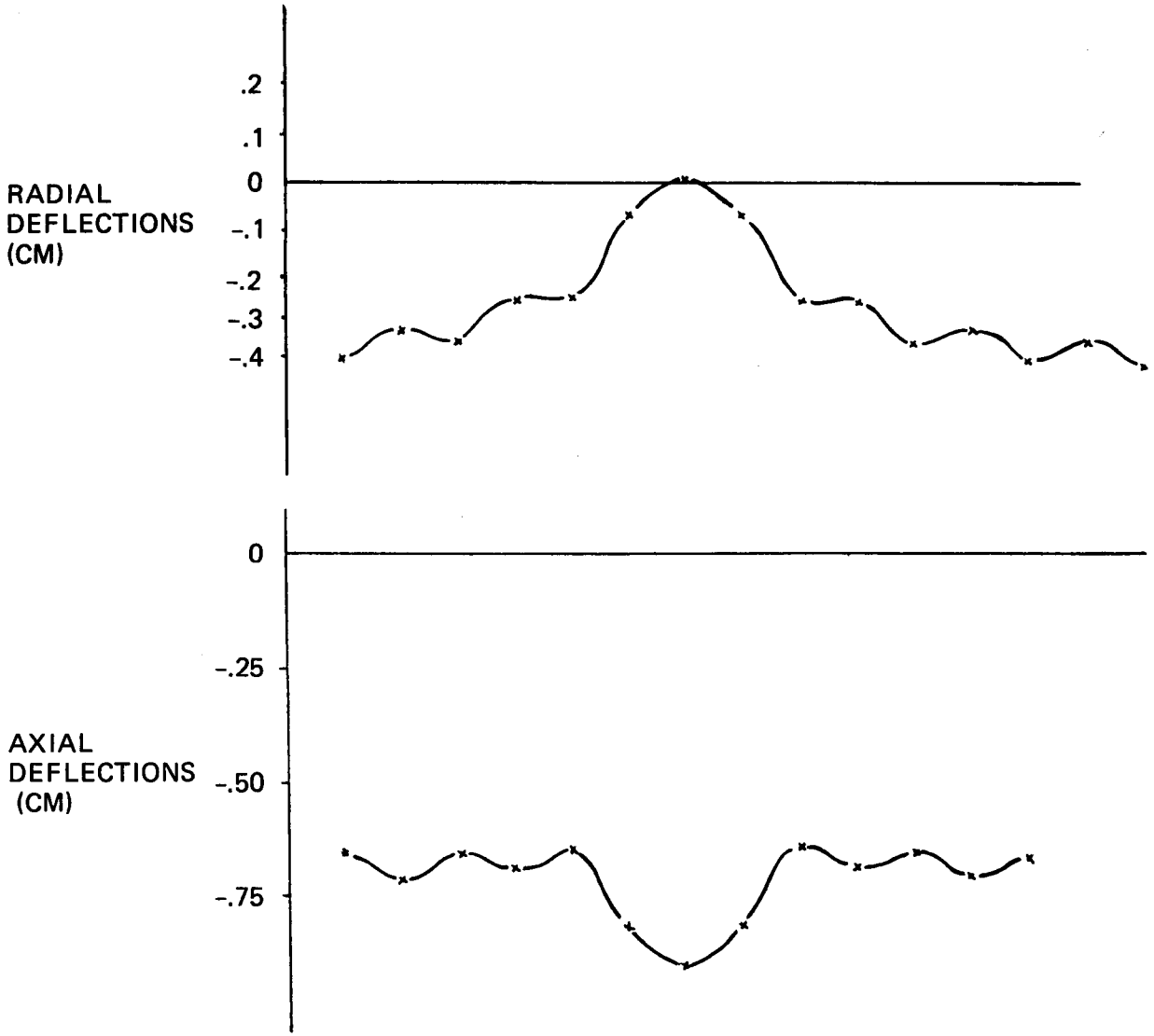

Fig. 21 Deployable Antenna Deflections with Forestay Removed

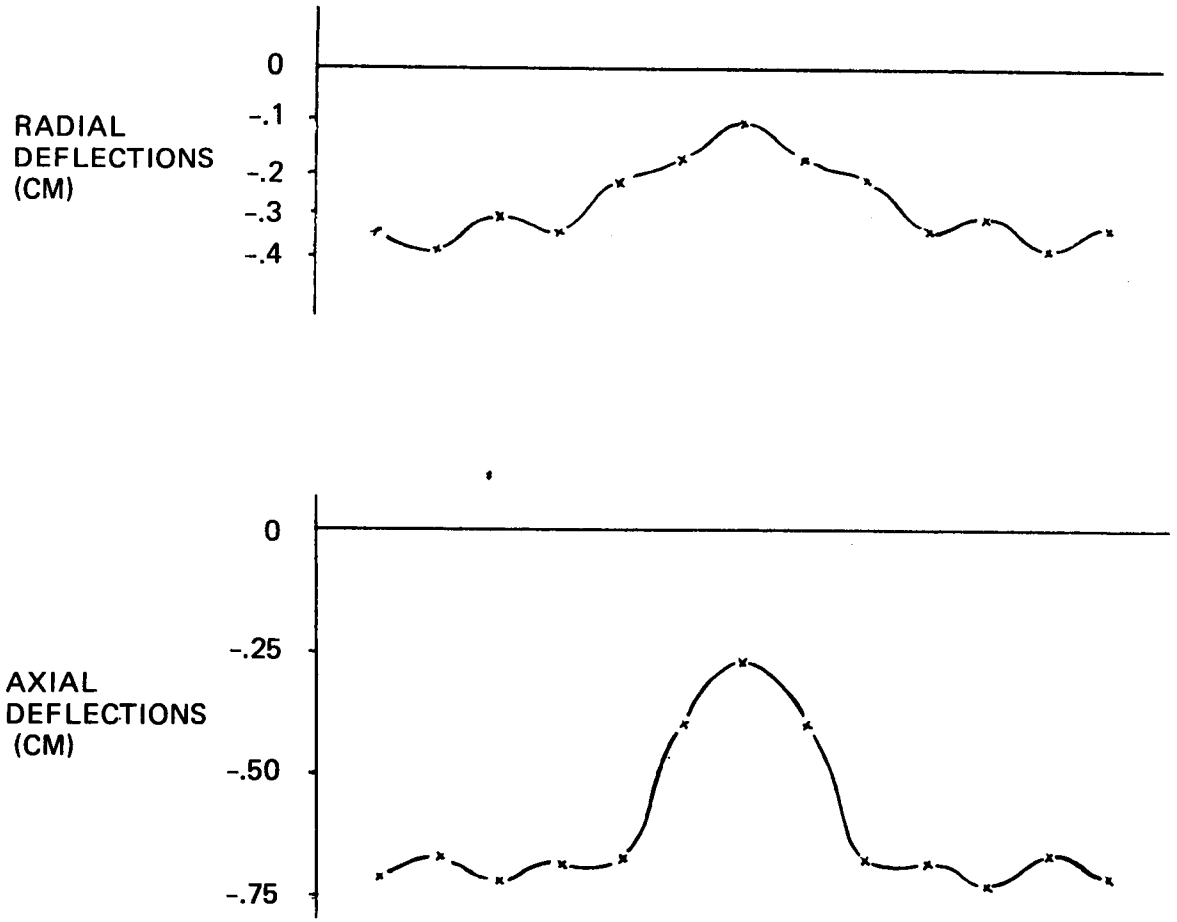

Fig. 22 Deployable Antenna Deflections with Backstay Removed

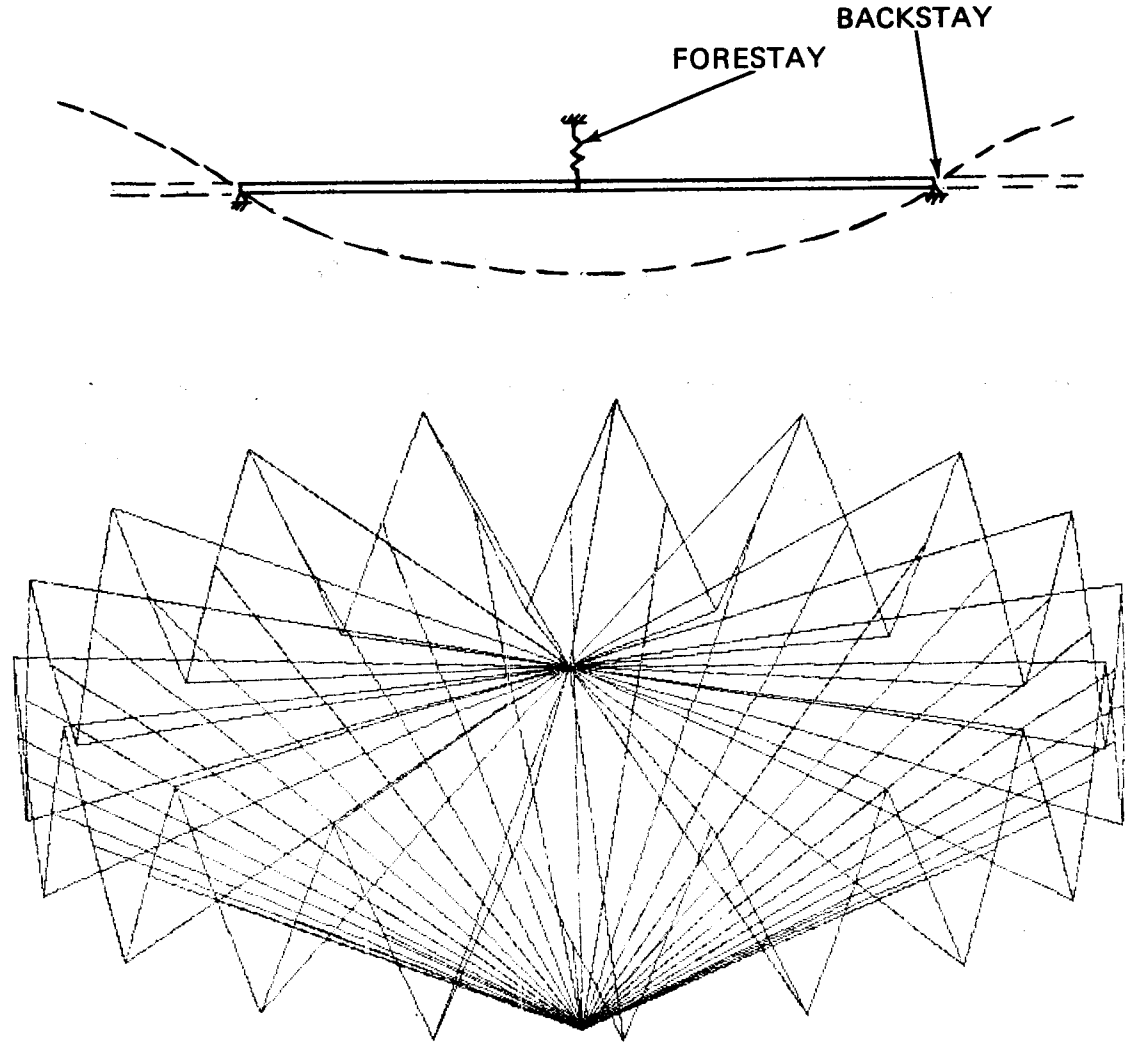

Fig. 23 Buckling Mode Shape of Antenna

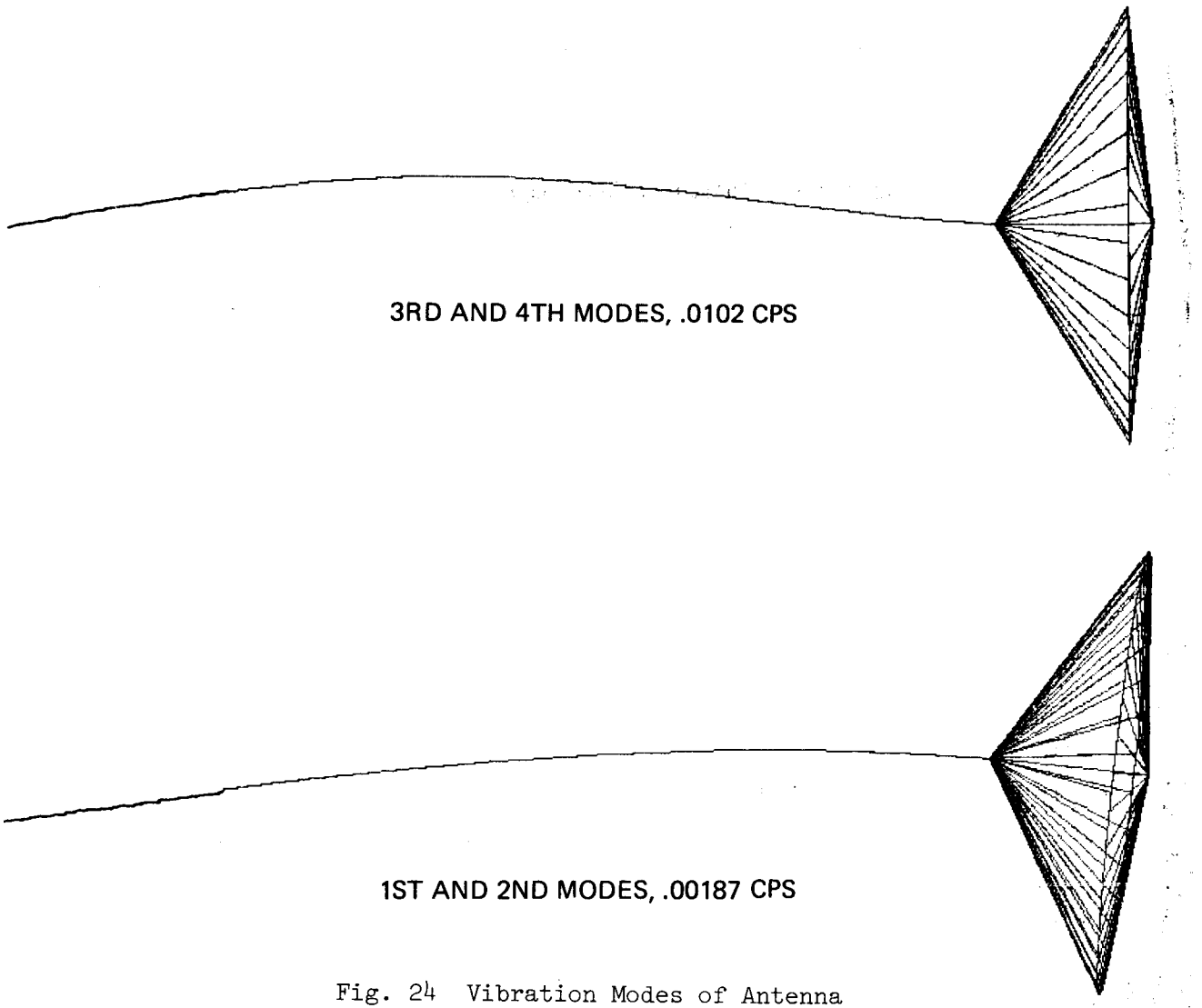

Fig. 24 Vibration Modes of Antenna

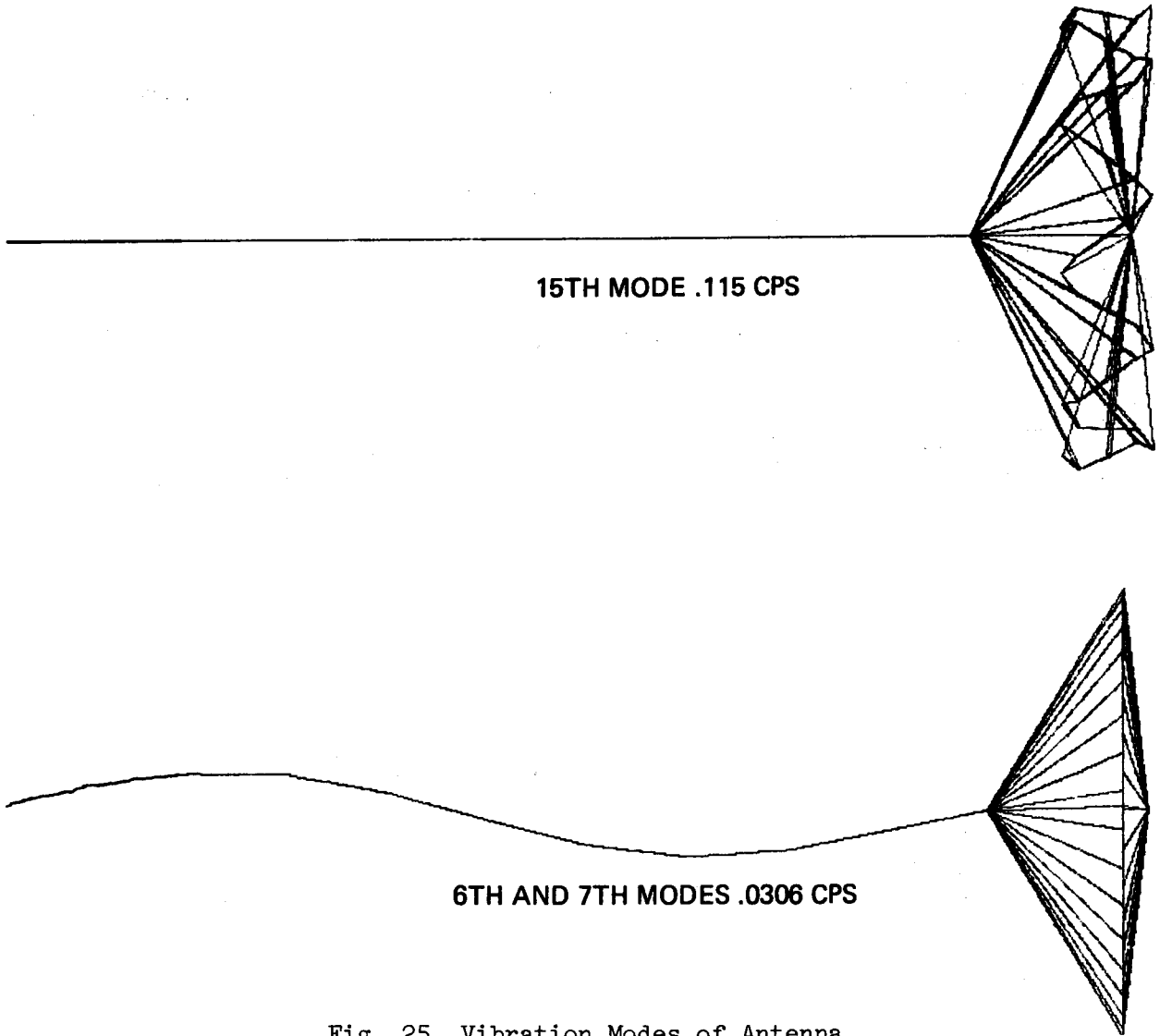

Fig. 25 Vibration Modes of Antenna